Accelerating structure-function mapping using the ViVa webtool to mine natural variation

Morgan O. Hamm[1], Britney L. Moss[2], Alexander R. Leydon[1], Hardik P. Gala[1], Amy Lanctot[1], Román Ramos[1], Hannah Klaeser[2], Andrew C. Lemmex[1], Mollye L. Zahler[1], Jennifer L. Nemhauser[1], R. Clay Wright[3]*

[1]Department of Biology, University of Washington, Seattle, WA, USA.

[2]Department of Biology, Whitman College, Walla Walla, WA, USA.

[3]Biological Systems Engineering, Virginia Tech, Blacksburg, VA, USA. Previous affiliation: Department of Biology, University of Washington, Seattle, WA, USA.

*Direct correspondence to: wrightrc@vt.edu.

2018-12-05

Thousands of sequenced genomes are now publicly available capturing a significant amount of natural variation within plant species; yet, much of this data remains inaccessible to researchers without significant bioinformatics experience. Here, we present a webtool called ViVa (Visualizing Variation) which aims to empower any researcher to take advantage of the amazing genetic resource collected in the *Arabidopsis thaliana* 1001 Genomes Project (http://1001genomes.org). ViVa facilitates data mining on the gene, gene family or gene network level. To test the utility and accessibility of ViVa, we assembled a team with a range of expertise within biology and bioinformatics to analyze the natural variation within the well-studied nuclear auxin signaling pathway. Our analysis has provided further confirmation of existing knowledge and has also helped generate new hypotheses regarding this well studied pathway. These results highlight how natural variation could be used to generate and test hypotheses about less studied gene families and networks, especially when paired with biochemical and genetic characterization. ViVa is also readily extensible to databases of interspecific genetic variation in plants as well as other organisms, such as the 3,000 Rice Genomes Project (http://snp-seek.irri.org/) and human genetic variation (https://www.ncbi.nlm.nih.gov/clinvar/).

Keywords: natural variation, Arabidopsis thaliana, genome diversity, structure, function, genotype, phenotype, bioconductor, bookdown, r

1 Introduction

2   The sequencing of the first *Arabidopsis thaliana* genome ushered in a new era of tool
3   development and systematic functional annotation of plant genes (The Arabidopsis
4   Genome Initiative 2000). Since that landmark effort, massive scaling of sequencing
5   technology has allowed for the survey of genomic variation in natural *Arabidopsis thaliana*
6   populations (Nordborg et al. 2005; Borevitz et al. 2007; Weigel and Mott 2009). This
7   valuable population genetics resource has led to several associations of genetic loci with
8   phenotypic traits and provided insights into how selective pressure has influenced the
9   evolution of plant genomes (Long et al. 2013; Atwell et al. 2010; Clark et al. 2007).

10   Beyond its utility in gene discovery and understanding genome evolution, natural genetic
11   variation provides a catalog of permissible polymorphisms that can facilitate the
12   connection of genotype to phenotype at the gene, gene family and network scales (Joly-
13   Lopez, Flowers, and Purugganan 2016). This is an especially critical resource in large gene
14   families where loss of function in individual genes may have little or no phenotypic effect
15   and directed allele replacement remains time and resource-intensive. Massively parallel
16   assays of variant effects in human clinical medicine stand to revolutionize genetic
17   diagnostics and personalized medicine (Starita et al. 2017; Gasperini, Starita, and Shendure
18   2016; Matreyek, Stephany, and Fowler 2017). We envision the use of plant natural
19   variation datasets as a tool to similarly revolutionize breeding and genetic engineering of
20   crop plants by rapidly advancing our understanding of genotype/function/phenotype
21   relationships. A proof-of-principle survey of a relatively small subset of natural variants
22   paired with a synthetic assay of gene function successfully mapped critical functional
23   domains of auxin receptors and identified new alleles which affect plant phenotype (Wright
24   et al. 2017).

25   Why is the survey of natural variants not as routine as a BLAST search or ordering T-DNA
26   insertion mutants? One reason may be the current requirement for a fairly high level of
27   bioinformatics expertise to extract the desired information from whole genome
28   resequencing datasets. While existing resources such as the 1001 Proteomes website (Joshi
29   et al. 2012) and ePlant (Waese et al. 2017) facilitate access to this data at the gene scale,
30   they do not provide summaries or visualizations of variation at the gene family and
31   network scales. To address this concern, we created ViVa: a webtool and R-package for
32   **Vi**sualizing **Va**riation, which allows plant molecular biologists of any level access to gene-
33   level data from the 1001 Genomes database. Using ViVa researchers may: 1) Identify
34   polymorphisms to facilitate biochemical assays of variant effects (Starita et al. 2017;
35   Wright et al. 2017); 2) Produce family-wise alignments of variants to facilitate *de novo*
36   functional domain identification (Melamed et al. 2015); 3) Generate lists of accessions
37   containing polymorphisms to facilitate phenotypic analysis of gene variant effects (Park et
38   al. 2017); and 4) Quantify metrics of genetic diversity to facilitate the study of gene, gene
39   family and network evolution (Delker et al. 2010; Kliebenstein 2008).

Results and Discussion

An overview of ViVa

ViVa, in this first iteration, is meant to visualize natural variation in the coding sequences of genes. Non-coding sequence variation is intentionally excluded from the analysis tools. This reflects challenges both in alignment of non-coding sequences and the increased difficulty in assessing variation in these regions (Alexandre et al. 2018).

The development version of ViVa can be accessed as a Docker container https://hub.docker.com/r/wrightrc/r1001genomes/ or as an R-package at https://github.com/wrightrc/r1001genomes. ViVa will be hosted at https://www.plantsynbiolab.bse.vt.edu/ViVa/ upon release.

1

Figure 1 **Key elements of the webtool** *(a) The first section contains two collapsible panels, Gene Select and Annotation Files, which are used to input information about the genes to be investigated. (b) The SNP Stats tab provides gene-structure level counts and statistics on SNPs. (c) The Diversity Plot tab plots the nucleotide diversity of SNP sites along the length of the coding region of a selected gene. (d) The SNP Mapping tab plots accessions on a world*

1 *map colored according to the selected set of SNPs. (e) The SNP Browser tab allows variants*
2 *and accessions to be filtered by any combination of text and numeric fields. (f) The Alignments*
3 *tab aligns DNA and amino acid sequences of homologous genes, and colors sequence elements*
4 *based on SNPs and annotations.*

Gene Select and Annotation Files

6 At the top of the ViVa webtool are two collapsible panels used for entering the genes to
7 query and custom annotations for those genes (Figure 1a). The Gene Select panel permits
8 gene input by either typing in the genes' AGI/TAIR locus identifiers, or uploading a .csv file.
9 The Annotation Files panel is optionally used to upload an annotation file containing
10 coordinates of domains, mutations, or any other sequence knowledge that will be plotted
11 on some of the tabs of the webtools analysis section.

12 Below the data input section, the rest of the webtool is divided into several tabs containing
13 the interactive output of the program.

SNP Stats: Summary of gene information, structure, and diversity

15 The SNP Stats tab provides general information on the gene transcripts being queried, as
16 well as calculated counts/statistics on the content of variants found in the sample
17 population (Figure 1b). The first table of this section is basic information about the
18 transcripts, including TAIR locus and symbol, the chromosomal start and end position and
19 the transcript length. This information was collected from the Araport11 Official Release
20 (06/2016) annotation dataset (Cheng et al. 2017).

21 The next two tables provide counts of SNPs across the gene body for each transcript. The
22 Total Polymorphism Counts table provides the total number of observations of non-
23 reference allele counts of each variant type (the Col-0 accession TAIR9 genome is the
24 reference genome for this dataset). The Unique Allele Count table only counts the number
25 of unique variants and alleles within the population of accessions (*e.g.* if multiple
26 accessions have the same variant allele, that allele will only be counted once).

27 The Nucleotide Diversity Statistics table provides a nucleotide diversity statistic (π) for the
28 transcript and the coding sequence of each gene (Nei and Li 1979). Nucleotide diversity is
29 also calculated for the set of only synonymous (π_S) and only non-synonymous sites (π_N).
30 The ratio of the presence of non-synonymous to synonymous polymorphism provides a
31 measure of the potential for functional diversity (Firnberg and Ostermeier 2013;
32 Whitehead et al. 2012). We present π_N/π_S here as an correlate for functional diversity
33 throughout ViVa (Nelson, Moncla, and Hughes 2015; Hughes et al. 2000). While imperfect,
34 this metric may be suggestive of functional constraint when $\pi_N/\pi_S << 1$ and functional
35 diversity when $\pi_N/\pi_S >> 1$ (Hughes 1999).

Diversity plot: Visualize allelic diversity across the coding sequence

37 The Diversity Plot tab shows the nucleotide diversity of each variant in the coding region of
38 a selected gene (Figure 1c). Although the X-axis is marked by codon number from the N-
39 terminus for interpretability, the diversity values are based on single nucleotide sites. The

1   colors of markers on the plot identify the effect of the polymorphism. If annotation files are
2   provided, the background of the plot will be color coded by the annotated regions. If points
3   on the plot are selected by clicking and dragging a box over them, the data for the selected
4   points will appear in the grey box below the plot. Below this is a complete data table
5   containing all points on the plot which can be downloaded as a .csv file. This tab allows
6   users to identify regions of high diversity as well as isolate polymorphisms that may affect
7   gene function and exist in multiple accessions, facilitating phenotypic analysis.

SNP Mapping: View distributions of SNPs across the globe

9   The SNP Mapping tab plots the accessions collection locations on a world map, and colors
10 the points based on selected variant alleles (Figure 1d). After selecting the genes and
11 filtering on the SNP type and level of nucleotide diversity, a group of checkboxes becomes
12 available to select variant alleles to display on the map. The variant alleles are labeled with
13 the Transcript_ID and Amino_Acid_Change fields, in the form
14 [Transcript_ID|Amino_Acid_Change]. After selecting the variant alleles and updating the
15 map, the accessions on the map will be colored by each present unique combination of the
16 selected alleles. Below the map is a table containing the accession details for all mapped
17 accessions. This tab may help users formulate hypotheses about the relatedness of
18 accessions sharing a common allele and environments in which that allele may be
19 favorable.

SNP Browser: Filter and search for variants

21 The SNP Browser tab provides a way to search and filter the variant data by different fields
22 (Figure 1e). After selecting the transcripts to include, a number of filters can be applied to
23 the dataset to match text values (e.g. gene name or variant effect), or set minimum and
24 maximum limits on the values of numeric fields (e.g. nucleotide diversity). When these
25 filters are applied, the table below will update to only contain rows meeting the criteria for
26 all filters. This tab can be useful for identifying all accessions with a particular SNP allele, or
27 any non-reference alleles in a particular region of a gene that may not have been easily
28 accessible in another tab.

Alignments: Visualize SNPs on alignments of homologous genes

30 The Alignments tab provides DNA and amino acid sequence alignments of selected genes,
31 colored according to the variant allele with the strongest functional effect at each position
32 (Figure 1f and 2). The content of this tab is most useful if the selected genes are all family
33 members or have significant sequence homology. If annotation files are uploaded, the
34 background of the sequences will be colored by annotation region. Hovering the cursor
35 over variants will provide additional details about the alleles present at that locus. This tab
36 facilitates family-wise analysis of functional conservation, allowing users to identify
37 potential functional regions and alleles which may be useful in deciphering this function.

Gene Tree: Visualize functional diversity and sequence divergence of a gene family

The Gene Tree tab provides a neighbor joining tree (or uploaded tree created by the user) for the selected genes with the tips of the tree mapped with predicted functional diversity as represented by π_N/π_S in the 1001 Genomes dataset (Figure 3). This tab allows users to generate hypotheses regarding functional diversity and redundancy within the context of the predicted evolution of the gene family.

ViVa R package: Programmatic access to ViVa's functionality

All of the functionalities of the ViVa webtool are implemented through function calls to the ViVa R package. In addition to being able to generate the same sets of figures and tables as in the webtool, users of the R package also gain direct access to the underlying data structures, providing greater control over parameters when processing and visualizing the data. The ViVa R package can be found at https://github.com/wrightrc/r1001genomes and can be installed in your R environment via the `devtools` package:
`devtools::install_github("wrightrc/r1001genomes")`.

Visualizing Variation within the auxin signaling pathway

To test the usability and accessibility of ViVa, we assembled a group of alpha testers comprising postdoctoral, graduate, and undergraduate researchers at a research university (University of Washington) and at a primarily-undergraduate institution (Whitman College). Our testers focused their investigation of natural variation on the nuclear auxin signaling pathway. We selected this signaling pathway for multiple reasons including a wealth of functional data and solved structures of several domains or entire proteins. Using this exitsting knowledge, we were able to qualitatively assess the predictive ability of the ViVa modules. Summary information about each nuclear auxin signaling gene family examined can be found in the Supplemental Data. Below, we describe the results for the *Aux/IAA* family in more detail.

In most cases, natural selection is expected to minimize the persistence of nonsynonymous mutations in sequences that encode critical functional domains relative to their persistence in non-critical domains (Hughes et al. 2000). Therefore, we reasoned that scanning gene coding sequences for regions of relatively low nonsynonymous diversity should highlight functional domains. This general principle can be seen clearly in the analysis of the *Aux/IAA* family of transcriptional co-repressors/co-receptors. Aux/IAAs have three major domains. Domain I contains an EAR motif that facilitates interaction with TOPLESS (TPL) and TOPLESS-related (TPR) transcriptional repressors (Tiwari, Hagen, and Guilfoyle 2004; Szemenyei, Hannon, and Long 2008). Domain II, the degron, facilitates interactions with the TIR1/AFB receptors in the presence of auxin (Tan et al. 2007). Domain III (which was originally considered domains III and IV) is a PB1 domain and facilitates interactions with the ARF transcription factors (Ulmasov et al. 1997; Guilfoyle and Hagen 2012; Nanao et al. 2014; Korasick et al. 2014). The EAR motif and degron can be readily identified by the drop in nonsynonymous variation, as visualized by the lack of stronger functional effects in Figure 2. The PB1 domain is not as readily identified, perhaps because the multiple

1 contributing residues are spread out in linear sequence space. It is worth noting that the
2 charged residues that facilitate electrostatic PB1-PB1 interaction show little variation.

3
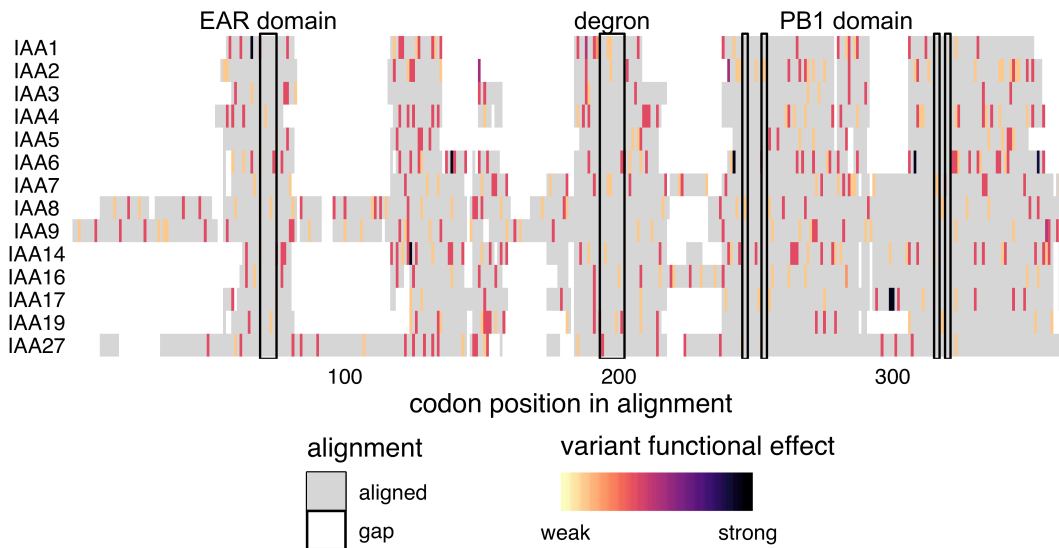
Figure 2 **Canonical Aux/IAAs have conserved Degron and EAR motifs.** *Protein sequences*
were aligned with DECIPHER (Wright 2015) and variants were mapped to this alignment and
colored according to the predicted functional effect of the allele of strongest effect at that
position, with light colors having weaker effects on function and darker colors stronger
effects. Red indicates missense variants. Color scale is explained in Methods.

9   Natural variation also provides a means to study how gene families are evolving. To do this,
10 we used ViVa to map onto the Aux/IAA phylogenetic tree the diversity at nonsynonymous
11 variant sites relative to synonymous sites (Figure 3). This visualization enables
12 straightforward comparison of rates of recent functional divergence within the context of
13 rates of sequence divergence across the entire gene family. By comparing nonsynonymous
14 diversity gene clades can be identified that are likely to exhibit high rates of functional
15 conservation and possible redundancy or conversely, where there is a possibility for recent
16 emergent novel function or pseudogenization.

17 Previous research has found evidence of both broad genetic redundancy among the
18 *Aux/IAAs* and also specificity within closely related pairs or groups of Aux/IAA proteins
19 (Overvoorde et al. 2005; Winkler et al. 2017). For example, the *iaa8-1 iaa9-1* double mutant
20 and the *iaa5-1 iaa6-1 iaa19-1* triple mutant have wild-type phenotypes (Overvoorde et al.
21 2005), yet the *IAA6/IAA19* sister pair has significant differences in expression patterns,
22 protein abundances and functions suggesting they have undergone functional
23 specialization since their divergence (Winkler et al. 2017). A closer examination of the
24 *IAA19* and *IAA6* pair within *Brassicaceae* found evidence for positive selection and possible
25 subfunctionalization of *IAA6* relative to *IAA19* (Winkler et al. 2017). Consistent with these
26 results, ViVa revealed higher conservation for *IAA19* ($\pi_N/\pi_S = 0.55$) compared to *IAA6*
27 ($\pi_N/\pi_S = 2.3$) (Figure 3), and also detected high nonsynonymous diversity within the same

8

1   regions of *IAA6* as seen by Winkler et al. (Figure 8). This pattern—one sister showing high
2   nonsynonymous diversity while the other sister was more conserved—was observed
3   frequently across the *Aux/IAA* as well as the *AFB* and *ARF* families (Figure 5 and 11),
4   suggesting this could be a recurring feature in the evolution of these families supporting
5   the large diversity in auxin functions.
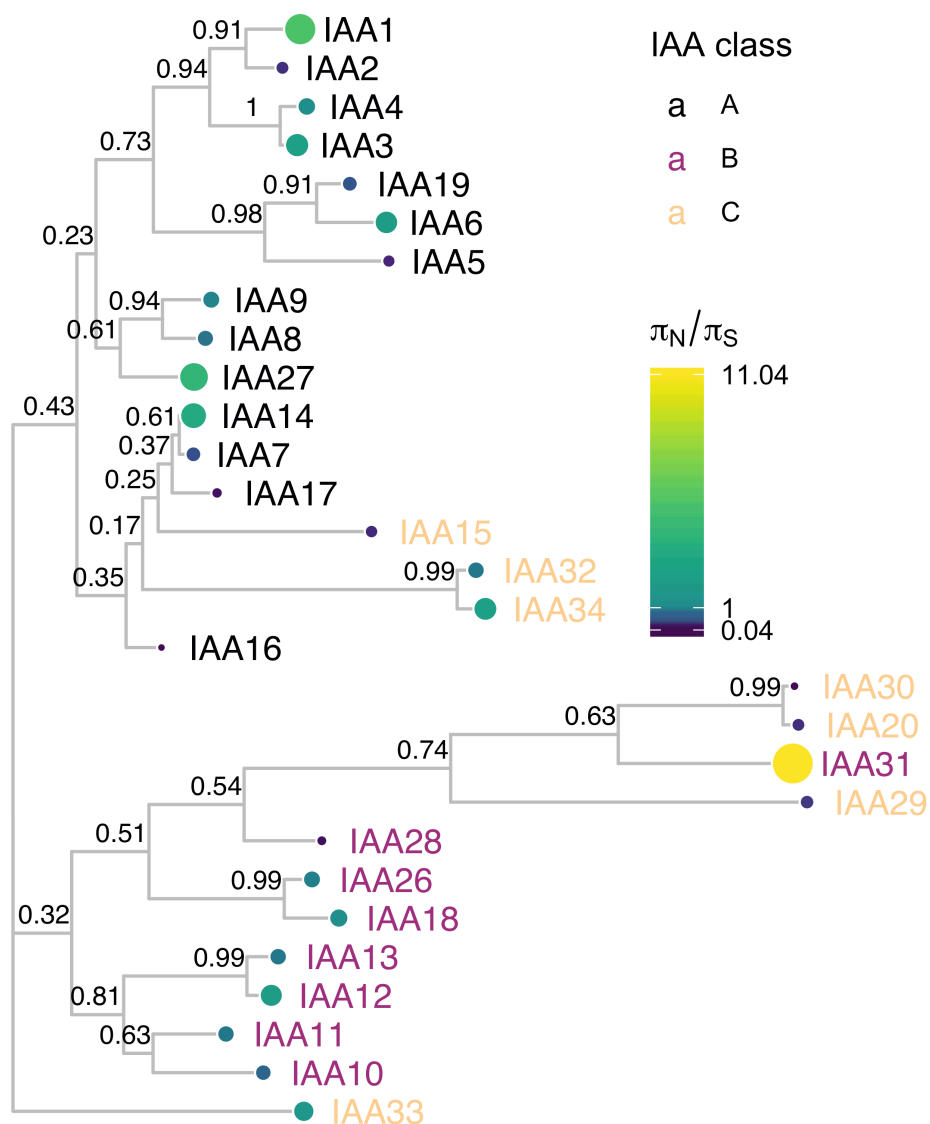
6

7   *Figure 3 **IAA protein sequence tree mapped with** π_N/π_S**.** Protein sequences were aligned*
8   *with DECIPHER (Wright 2015) and low information content regions were masked (Kück et al.*
9   *2010) prior to inferring a phylogeny (Ronquist and Huelsenbeck 2003). Tips of the tree are*
10   *mapped with circles of color and diameter proportional to π_N/π_S. π_N/π_S provides a*
11   *prediction of functional diversity. Nodes are labeled with the poster probability of monophyly.*

1   *There are two distinct clades of Aux/IAAs represented by the majority of the A and B classes. C*
2   *class Aux/IAAs are missing one or more of the canonical Aux/IAA domains.*

3   The *Aux/IAA* phylogeny clusters into two distinct clades represented by the A and B classes
4   (Remington et al. 2004). The C class Aux/IAAs are missing one or more of the canonical
5   Aux/IAA domains. We found notable exceptions to pattern of diversification and
6   conservation between sister pairs within the Class B *Aux/IAA* genes. The *IAA10/IAA11*,
7   *IAA18/IAA26*, and *IAA20/IAA30* pairs showed similar levels of nonsynonymous diversity.
8   For example, *IAA10* and *IAA11* both showed functional conservation (π_N/π_S of 0.80 and
9   0.67 respectively). In support of this strong conservation of both *IAA10* and *IAA11*, the
10 *Arabidopsis thaliana* ePlant browser indicates that *IAA10* and *IAA11* have almost identical
11 expression patterns (Waese et al. 2017). Together this evidence suggests a strong dosage
12 requirement for these genes or that they have taken on novel functions since their
13 emergence.

Conclusion

15 ViVa has allowed our team of testers from various skill levels and backgrounds to
16 meaningfully access the 1001 genomes dataset. The visualizations of natural variation
17 further supported much of the existing structure-function knowledge of this well studied
18 signaling pathway and facilitated the generation of new hypotheses. Application of ViVa to
19 less studied genes and gene families promises to yield more novel hypotheses, which can
20 be evaluated with mutagenesis and functional assays to glean novel structure/function
21 knowledge from this rich dataset.

22 ViVa results are intended to inform and inspire hypothesis generation, not be taken as
23 absolute evidence of trends in gene or gene family evolution. Among the cautions worth
24 noting in interpreting results are limitations of short-read sequencing that lead to regions
25 of missing data where low read quality may have prevented variant calls. We have assumed
26 these missing variants are reference alleles, leading to undercounting in ViVa's diversity
27 estimations. Recent advances in sequencing technologies have been combined to generate
28 extremely high quality genomes (Michael et al. 2018), and will reduce this source of
29 uncertainty in future resequencing datasets. Another limitation is that the geographic
30 coverage of accessions in the 1001 Genomes dataset is far from uniform, and thus diversity
31 scores may not accurately reflect the allelic distributions of the global *Arabidopsis thaliana*
32 population.

33 We hope that ViVa will advance understanding of genotype-phenotype relationships by
34 allowing all researchers access to large resequencing datasets. In the future, we intend to
35 expand ViVa beyond the plant genetics workhorse, *Arabidopsis thaliana*, to more
36 agriculturally relevant species with existing resequencing projects, such as rice (Wang et al.
37 2018) and soybean (Zhou et al. 2015). Indeed, the ViVa framework is readily adaptable to
38 any source of targeted resequencing data. If François Jacob's metaphor holds true, and
39 evolution is indeed a tinkerer and not an engineer (Jacob 1977), it is only by examining the
40 largest possible number of nature's solutions that we may eventually decipher the
41 principles constraining innovations in form and function.

1 Methods

2 Data Sources

3 Variant Data

4 Variant data was queried from the 1001 genomes project (http://1001genomes.org) via
5 URL requests to their API service (http://tools.1001genomes.org/api/index.html). These
6 queries returned subsets of the whole-genome variant call format (VCF) file as SnpEFF VCF
7 files. The whole-genome VCF file can be found on the project's website at
8 http://1001genomes.org/data/GMI-MPI/releases/v3.1/.

9 Germplasm Accession Information

10 A dataset of each of the 1135 accessions including CS stock numbers and geographic
11 location where the samples were collected was retrieved from the 1001 Genomes website
12 at http://1001genomes.org/accessions.html, via the download link at the bottom of the
13 page. This data file has been embedded in the R package as `accessions`.

14 Gene and Transcript Accession Information

15 Information on the genes and transcripts including chromosomal coordinates, start and
16 end location, and transcript length were pulled from Araport11 (Cheng et al. 2017). The
17 TAIR10 database, found at http://arabidopsis.org, was accessed via the `biomart` function,
18 using the biomaRt R-package. The Araport11 full genome general feature format file, which
19 can also be found on the TAIR website (https://www.arabidopsis.org/download/index-
20 auto.jsp?dir=%2Fdownload_files%2FGenes%2FAraport11_genome_release), has been
21 embedded in the R-package as GRanges object, `gr`. Gene identifiers used in this study are in
22 Table 1.

23 *Table 1 Full list of genes used in this study, by identifier, symbol and classification.*

Arabidopsis AGI locus identifier	Gene symbol	Clade/class
AT3G62980	TIR1	NA
AT4G03190	AFB1	NA
AT3G26810	AFB2	NA
AT1G12820	AFB3	NA
AT4G24390	AFB4	NA
AT5G49980	AFB5	NA
AT2G39940	COI1	NA
AT4G14560	IAA1	A
AT3G23030	IAA2	A
AT1G04240	IAA3	A
AT5G43700	IAA4	A

11

AT1G15580	IAA5	A
AT1G52830	IAA6	A
AT3G23050	IAA7	A
AT2G22670	IAA8	A
AT5G65670	IAA9	A
AT1G04100	IAA10	B
AT4G28640	IAA11	B
AT1G04550	IAA12	B
AT2G33310	IAA13	B
AT4G14550	IAA14	A
AT1G80390	IAA15	A
AT3G04730	IAA16	A
AT1G04250	IAA17	A
AT1G51950	IAA18	B
AT3G15540	IAA19	A
AT2G46990	IAA20	C
AT3G16500	IAA26	B
AT4G29080	IAA27	A
AT5G25890	IAA28	B
AT4G32280	IAA29	C
AT3G62100	IAA30	C
AT3G17600	IAA31	C
AT2G01200	IAA32	C
AT5G57420	IAA33	C
AT1G15050	IAA34	C
AT1G15750	TPL	NA
AT1G80490	TPR1	NA
AT3G16830	TPR2	NA
AT5G27030	TPR3	NA
AT3G15880	TPR4	NA
AT1G59750	ARF1	B
AT5G62000	ARF2	B
AT2G33860	ARF3	B
AT5G60450	ARF4	B
AT1G19850	ARF5	A
AT1G30330	ARF6	A

AT5G20730	ARF7	A
AT5G37020	ARF8	A
AT4G23980	ARF9	B
AT2G28350	ARF10	C
AT2G46530	ARF11	B
AT1G34310	ARF12	B
AT1G34170	ARF13	B
AT1G35540	ARF14	B
AT1G35520	ARF15	B
AT4G30080	ARF16	C
AT1G77850	ARF17	C
AT3G61830	ARF18	B
AT1G19220	ARF19	A
AT1G35240	ARF20	B
AT1G34410	ARF21	B
AT1G34390	ARF22	B
AT1G43950	ARF23	B

Ranking of variant functional effects

Alignments were colored according to the strongest effect variant allele occurring at any frequency at that position as reported in the SnpEFF "effect" field, per the scale in Figure 4.

1
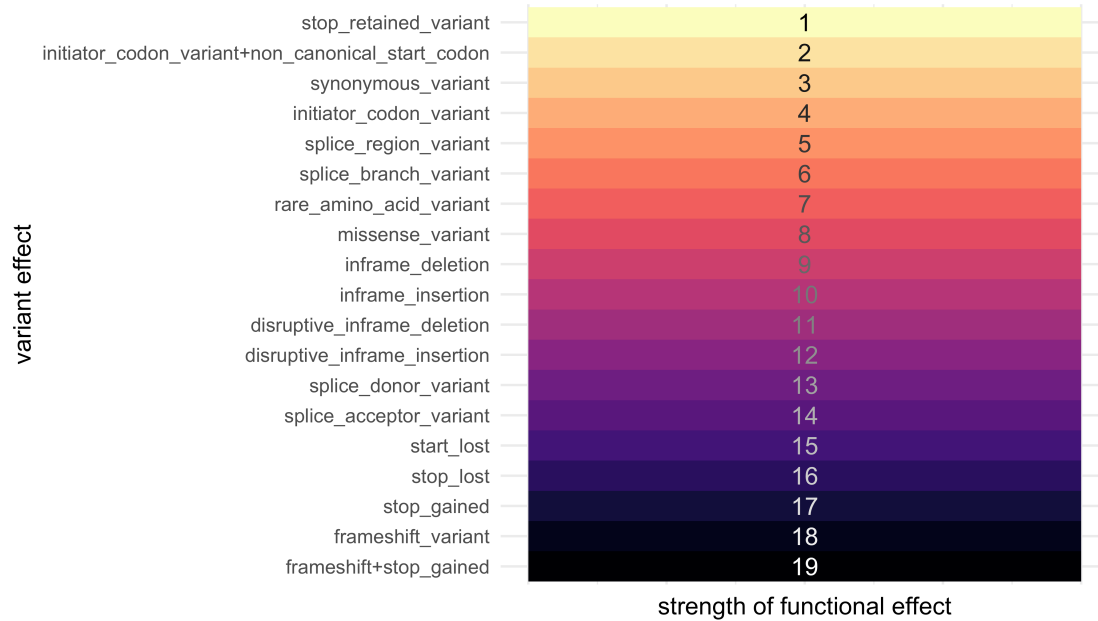
Figure 4 **Rank order of the strength of functional effects** *Effect classes were ordered by subjective prediction of average strength of effect on gene function. Strength was then assigned to each effect on an integer scale.*

Nucleotide Diversity Calculation

Nei and Li defined the nucleotide diversity statistic in their original paper as: "the average number of nucleotide differences per site between two randomly chosen DNA sequences" (Nei and Li 1979), and provided the equation:

$$\pi = \sum_{ij} x_i\, x_j \pi_{ij}. \qquad (1)$$

Where x_i is the frequency of the ith sequence in the population and π_{ij} is the number of sites that are different between the ith and jth sequence divided by sequence length.

A more general form, that treats each sequence in the population as unique can be written as:

$$\pi = \frac{1}{L*n^2}\sum_{i=1}^{n}\sum_{j=1}^{n}\sum_{k=1}^{L}\pi_{ijk} \qquad \pi_{ijk} = \begin{cases} 1 & \text{if} \quad N_{ik} \neq N_{jk} \\ 0 & \text{if} \quad N_{ik} = N_{jk} \end{cases} \qquad (2)$$

where N_{ik} is the nucleotide (A, T, C or G) at position k on the ith sequence of the population. L is the length of the sequence. Indels are excluded from the diversity calculation leading to a single L for the population. n is the total number of sequences in the population.

From this form we can re-arrange summations to the form below:

14

1

$$\pi = \frac{1}{L} \sum_{k=1}^{L} \pi_k \qquad \pi_k = \frac{1}{n^2} \sum_{i=1}^{n} \sum_{j=1}^{n} \pi_{ijk} \qquad (3)$$

2 where π_k can be thought of as the site-wise nucleotide diversity at position k, and is equal
3 to the nucleotide diversity of a sequence of length 1 at location k. We can calculate π_k for
4 each site, then average those over the sequence length to calculate π, the nucleotide
5 diversity of the sequence.

6 The function `Nucleotide_diversity` in the r1001genomes package calculates π_k for each
7 position in the gene or region that contains a variant. Note, π_k is equal to 0 at all locations
8 without variants. This is also what is displayed in the Diversity Plot tab of the webtool.

9 ## Detailed π_k calculation simplification.

10 The formula for π_k above requires comparing every sequence to every other sequence at
11 location k, however, we know there are only a few variant forms at each individual location.

12 So, we can revert back to using Nei and Li's original formula (1), modifying it slightly,
13 replacing x_i with $\frac{n_i}{n}$, n_i being the number of sequences in the population with nucleotide N_i
14 at location k:

15

$$\pi_k = \sum_{ij} \frac{n_i}{n} \frac{n_j}{n} \pi_{ij} = \frac{1}{n^2} \sum_{ij} n_i n_j \pi_{ij} \qquad \pi_{ij(k)} = \begin{cases} 1 & \text{if} \quad i \neq j \\ 0 & \text{if} \quad i = j \end{cases} \qquad (4)$$

16 Note that in equation (1) subscripts i and j are summed over all sequences in the
17 population, however in equation (4) i and j are only summed over unique variants at a
18 particular location k.

19 We will define $n_{!i} = n - n_i$ as the number of sequences different from i at position k. We
20 can also see that the summed term will be zero if $i = j$, and $n_i n_j$ if $i \neq j$. Therefore:

21

$$\pi_k = \frac{1}{n^2} \sum_{i} n_i n_{!i} \qquad (5)$$

22 Next we substitute our definition of $n_{!i}$:

23

$$\pi_k = \frac{1}{n^2} \sum_{i} n_i (n - n_i) \qquad (6)$$

24 Distributing and splitting summation yields:

25

$$\pi_k = \frac{1}{n^2} \left(n \sum_{i} n_i - \sum_{i} n_i^2 \right) \qquad (7)$$

26 Finally, summing $\sum_i n_i$ is equal to n:

15

$$\pi_k = \frac{1}{n^2}(n^2 - \sum_i n_i^2) \qquad (8)$$

This simplified form for π_k is used by the app, because the counts of unique variants at a single nucleotide location can easily be summarized in R.

Software

The r1001genomes package has many software dependencies on other R packages, a few of the key bioinformatics packages used are listed below.

biomaRt: used for accessing the TAIR10 database on arabidopsis.org

vcfR: used to read in the VCF files in a flat "tidy" format for easy manipulation

BSgenome: used as the source for the complete DNA string of the reference genome (Col-0).

DECIPHER: used to align nucleotide and amino acid sequences of homologous genes

GenomicFeatures: used for handling sequence annotations.

Biostrings: provides the underlying framework for the sequence manipulations used for generating and aligning sequences with BSgenome, Decipher, and GenomicFeatures

Other packages that were critical to building ViVa and/or writing this document include: (Paradis et al. 2018; R Core Team 2018; Müller 2018; Team 2018; Pagès et al. 2018; Xie 2018a; Ihaka et al. 2016; Wright 2018; Wickham, François, et al. 2018; Xie 2018b; Wickham 2018a; Aphalo 2018a; Wickham, Chang, et al. 2018; Aphalo 2018b; Wagih 2017; Arnold 2018; Yu and Lam 2018; Heibl 2014; Pagès, Aboyoun, and Lawrence 2018; Xie 2018c; Bache and Wickham 2014; Wickham 2016; Henry and Wickham 2018; Hamm and Wright 2018; Neuwirth 2014; Wickham, Hester, and Francois 2017; Wickham 2017a; Allaire, Ushey, and Tang 2018; Allaire et al. 2018; Müller et al. 2018; Pagès, Lawrence, and Aboyoun 2018; Wickham 2018b; Wickham 2018c; Müller and Wickham 2018; Wickham and Henry 2018; Wickham 2017b; Yu 2018; Garnier 2018a; Garnier 2018b; Temple Lang and CRAN Team 2018; Pagès and Aboyoun 2018)

16

1 Acknowledgements

10 Supplemental Data

11 *TIR1/AFB* genes

12 Auxin acts by binding to receptors (Auxin-signaling F-Boxes, or AFBs) that in turn target
13 co-repressors (Aux/IAAs) for degradation. The six auxin receptor genes in the model plant
14 *Arabidopsis thaliana*, *TIR1* and *AFB1-5*, evolved through gene duplication and
15 diversification early in the history of vascular plants (Parry et al. 2009). The rate of co-
16 repressor degradation is determined by the identity of both the receptor and co-repressor
17 (Havens et al. 2012), and this rate sets the pace of lateral root development (Guseman et al.
18 2015).

19 All members of this family have been shown to bind auxin and Aux/IAA proteins. However,
20 AFB1 has drastically reduced ability to assemble into an SCF complex, due to the
21 substitution E8K in its F-box domain, preventing it from inducing degradation of Aux/IAAs
22 (Yu et al. 2015). This lack of SCF formation may allow for the high and ubiquitous AFB1
23 accumulation observed in *Arabidopsis* tissues (Parry et al. 2009). Higher order receptor
24 mutants in the family containing *afb1* mutants suggest that *AFB1* has a moderate positive
25 effect on auxin signaling (Dharmasiri et al. 2005). Additionally, AFB4 and AFB5 have been
26 shown to preferentially and functionally bind the synthetic auxin picloram, while other
27 family members preferentially bind indole-3-acetic acid (Prigge et al. 2016). Interestingly,
28 the strength and rate with which TIR1/AFBs are able to bind and mark Aux/IAAs for
29 degradation are variable (Calderón Villalobos et al. 2012; Havens et al. 2012). AFB2
30 induces the degradation of certain Aux/IAA proteins at a faster rate than TIR1, suggesting
31 some functional specificity has arisen since the initial duplication between the *TIR1/AFB1*
32 and *AFB2/AFB3* clades.
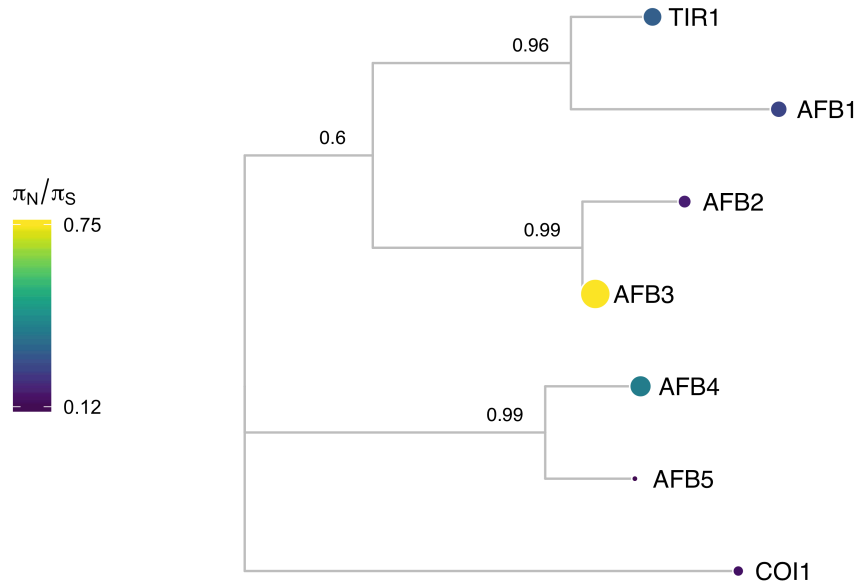
1

2   *Figure 5 **AFB protein sequence tree mapped with** π_N/π_S**.** Protein sequences were aligned*
3   *with DECIPHER (Wright 2015) and low information content regions were masked with*
4   *Aliscore (Kück et al. 2010) prior to inferring a phylogeny with MrBayes (Ronquist and*
5   *Huelsenbeck 2003). Tips of the tree are mapped with circles of diameter proportional to*
6   *π_N/π_S and also are colored according to π_N/π_S. Nodes are labeled with the posterior*
7   *probability of monophyly.*

8   Examining the natural sequence variation across the *AFB* family 5 revealed that *TIR1* and
9   *AFB1* both had very low nonsynonymous diversity, hinting at their likely functional
10 importance and bringing in to question the inconclusive role of *AFB1* in auxin signaling.
11 *AFB3* and *AFB4* had higher nonsynonymous diversity, while their sister genes, *AFB2* and
12 *AFB5* were more conserved. This matches our current understanding of *AFB3* as playing a
13 minor role in the auxin signaling pathway (Dharmasiri et al. 2005) and suggests *AFB4* may
14 be undergoing pseudogenization, especially when paired with its low expression levels
15 (Prigge et al. 2016).

18

1
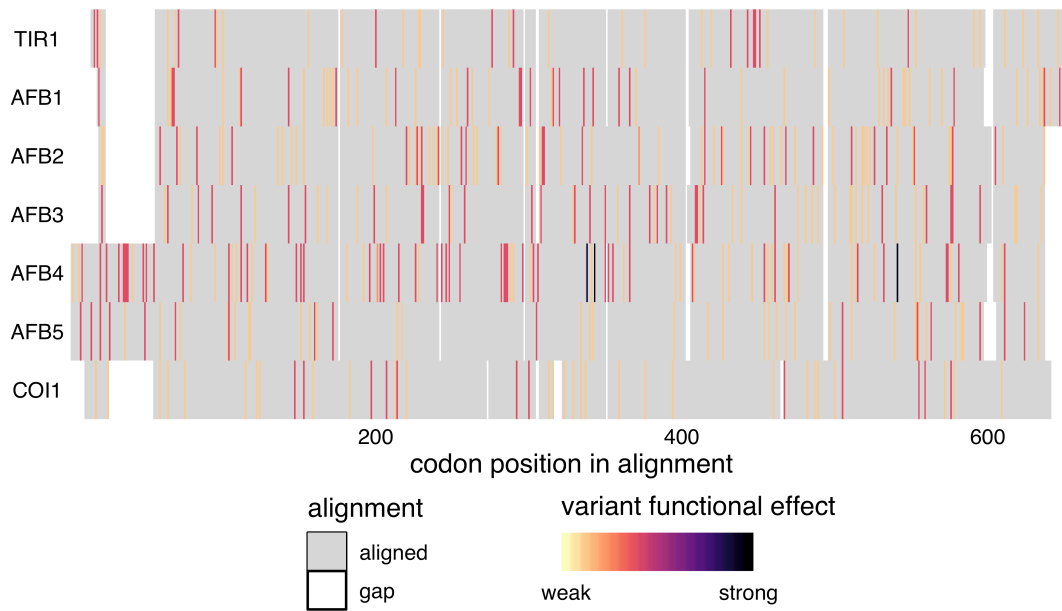
*Figure 6 **Alignment of the AFB family** Protein sequences were aligned with DECIPHER (Wright 2015) and variants were mapped to this alignment and colored according to the predicted functional effect of the allele of strongest effect at that position, with light colors having weaker effects on function and darker colors stronger effects. Red indicates missense variants. Color scale is explained in Methods.*

Although most known functional regions are highly conserved in *AFB1*, there are some nonsynonymous polymorphism in the oligomerization domain that are only present in single accessions (F125E in Can-0 and I163N in Pu2-23). Mutations in this domain of *TIR1* frequently have a semidominant effect on root phenotypes (Dezfulian et al. 2016; Wright et al. 2017). Characterization of this allele and accession may help determine the role of *AFB1* in this pathway.

The AFB4 and AFB5 receptors have an N-terminal extension prior to their F-box domains. This extension had very high nonsynonymous diversity (Figure 6, suggesting that this extension does not play an important functional role in these proteins. Additionally, two frameshift variants and one stop-gained variant were observed in *AFB4* supporting its pseudogenization.

Aux/IAA genes

For simplicity we have included only the alignment of the class A Aux/IAAs in the main manuscript. For completion we include here the complete alignment of the family.

19

1

Figure 7 **Alignment of the complete Aux/IAA family.** *Protein sequences were aligned with DECIPHER (Wright 2015) and variants were mapped to this alignment and colored according to the predicted functional effect of the allele of strongest effect at that position, with light colors having weaker effects on function and darker colors stronger effects. Red indicates missense variants. Color scale is explained in Methods.*

1

Figure 8 **IAA6 diversity plot** *Nucleotide diversity of variant positions throughout the IAA6 coding sequence are plotted and colored according to the effect of the variant alleles at each position. The region of positive selection identified by Winkler et al. is highlighed.*

TPL/TPR genes

The auxin signaling pathway utilizes the TOPLESS (TPL) and TOPLESS-related (TPR) family of Gro/TLE/TUP1 type co-repressor proteins to maintain auxin responsive genes in a transcriptionally-repressed state in the absence of auxin (Szemenyei, Hannon, and Long 2008). In *Arabidopsis thaliana* the five member *TPL/TPR* family includes *TPL* and *TPR1-4*. The resulting proteins are comprised of three structural domains: an N-terminal TPL domain and two WD-40 domains (Long et al. 2006). TPL/TPR proteins are recruited to the AUX/IAA proteins through interaction with the conserved Ethylene-responsive element binding factor-associated amphiphilic repression (EAR) domain (Szemenyei, Hannon, and Long 2008). Canonical EAR domains have the amino acid sequence LxLxL, as found in most AUX/IAAs (Overvoorde et al. 2005). TPL/TPR co-repressors bind EAR domains via their C-terminal to LisH (CTLH) domains found near their N-termini (citations of pre-structure founding papers/reviews). Recent structural analyses of the TPL N-terminal domain have highlighted the precise interaction interface between TPL and AUX/IAA EAR domains, as well as the TPL-TPL dimerization and tetramerization motifs (Martin-Arevalillo et al. 2017; Ke et al. 2015). The residues required for higher-order multimers of TPL tetramers have also been identified (Ma et al. 2017). Additional interactions with transcriptional regulation and chromatin modifying machinery are likely mediated by two tandem beta propeller domains of TPL/TPRs.

The TOPLESS co-repressor family generally exhibits a high level of sequence conservation at the amino acid sequence level across resequenced *Arabidopsis thaliana* accessions, with all π_N/π_S values below 1 (Figure 9). The closely related *TPL* and *TPR1* have the highest

21

1   π_N/π_S values, suggesting that these these two related genes tolerate a higher degree of
2   sequence and potentially functional diversity compared to *TPR2/3/4*. The N-terminal TPL
3   domain of the TPL/TPR family is particularly conserved. All nonsynonymous
4   polymorphisms observed in this region are either in the coils between helices or are highly
5   conservative mutations within helices (i.e. valine to isoleucine), which would be predicted
6   to exhibit little effect on folding and function.
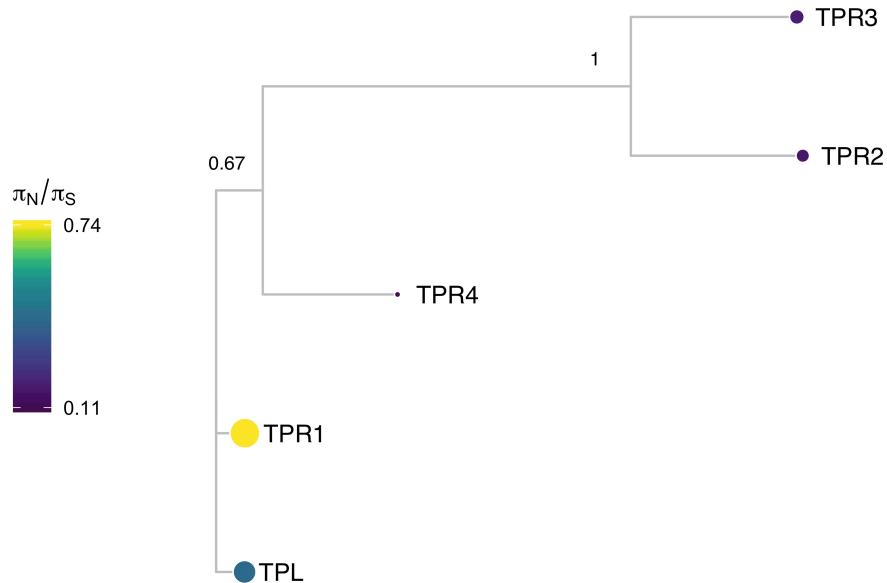
7

8   *Figure 9* **TPL protein sequence tree mapped with** π_N/π_S**.** *Protein sequences were aligned*
9   *with DECIPHER (Wright 2015) and low information content regions were masked with*
10 *Aliscore (Kück et al. 2010) prior to inferring a phylogeny with MrBayes (Ronquist and*
11 *Huelsenbeck 2003). Tips of the tree are mapped with circles of diameter proportional to*
12 π_N/π_S *and also are colored according to* π_N/π_S*. Nodes are labeled with the poster probability*
13 *of monophyly.*

14 The high degree of conservation in the entire N-terminal domain underscores its
15 importance in TPL/TPR function (Figure 10. For example, the initial *tpl-1* mutation
16 (N176H) in the ninth helix is a dominant gain-of-function allele (Long et al. 2006), which is
17 capable of binding wild-type TPL protein and inducing protein aggregation (Ma et al.
18 2017). It is therefore understandable that this helix had very low diversity as
19 nonsynonymous variants in this domain could act in a dominant negative fashion.

22

1
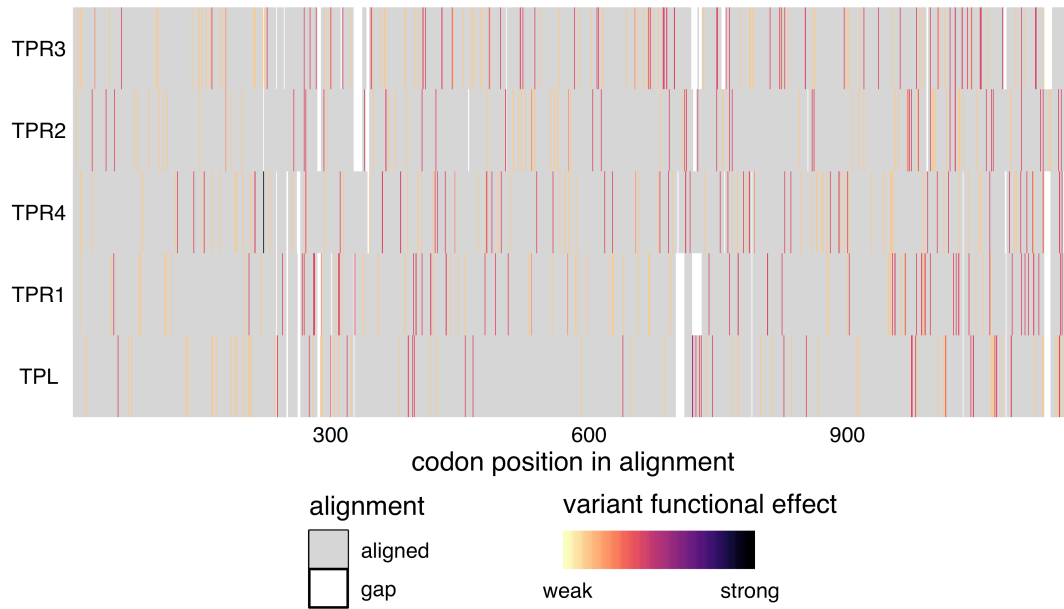
*Figure 10 **Alignment of the TPL/TPR family.** Protein sequences were aligned with DECIPHER (Wright 2015) and variants were mapped to this alignment and colored according to the predicted functional effect of the allele of strongest effect at that position, with light colors having weaker effects on function and darker colors stronger effects. Red indicates missense variants. Color scale is explained in Methods.*

ARF genes

Auxin response is mediated by the auxin responsive transcription factors (ARFs). There are 23 *ARF*s in *Arabidopsis thaliana* that are divided into three phylogenetic classes. Class A ARFs (ARF5, ARF6, ARF7, ARF8 and ARF19) activate transcription. These ARFs have a glutamine-rich region in the middle of the protein that may mediate activation (Guilfoyle and Hagen 2007). It has recently been shown that the middle region of ARF5 interacts with the SWI/SNF chromatin remodeling ATPases BRAMA and SPLAYED, possibly to reduce nucleosome occupancy and allow for the recruitment of transcription machinery (Wu et al. 2015). Additionally, ARF7 interacts with Mediator subunits, directly tethering transcriptional activation machinery to its binding sites in the chromosome (Ito et al. 2016). Class B and C *ARF*s are historically categorized as repressor *ARF*s, though the mechanism through which they confer repression has not been identified. Their middle regions tend to be proline- and serine-rich.

Canonical ARFs are comprised of three major domains. Recent crystallization of these domains have informed structure-function analysis of the ARFs (Boer et al. 2014; Korasick et al. 2014; Nanao et al. 2014). These domains are conserved throughout land plants (Mutte et al. 2018). ARFs share an N-terminal B3 DNA binding domain. Flanking this DNA-binding domain is a dimerization domain, which folds up into a single "taco-shaped" domain to allow for dimerization between ARFs. There is an auxiliary domain that immediately

23

1 follows and interacts with the dimerization domain. The middle region is the most variable
2 between ARFs, as mentioned above, but is characterized by repetitive units of glutamine
3 (class A), serine, or proline residues (classes B and C). The C-terminal domain of canonical
4 ARFs is a PB1 protein-protein interaction domain mediating interactions among ARFs,
5 between ARFs and other transcription factors, and between ARFs and the Aux/IAA
6 repressors. This interaction domain was recently characterized as a Phox and Bem1 (PB1)
7 domain, which is comprised of a positive and negative face with conserved basic and acidic
8 residues, respectively (Korasick et al. 2014; Nanao et al. 2014). The dipolar nature of the
9 PB1 domain may mediate multimerization by the pairwise interaction of these faces on
10 different proteins as the ARF7 PB1 domain was crystallized as a multimer (Korasick et al.
11 2014). However, it is unclear whether ARF multimerization occurs or plays a significant
12 role *in vivo*. Interfering with ARF dimerization in either the DNA-binding proximal
13 dimerization domain or the PB1 domain decreases the ability of class A ARFs to activate
14 transcription in a heterologous yeast system (Pierre-Jerome et al. 2016).

15 While domain architecture is broadly conserved among the ARFs, there are exceptional
16 cases. Three ARFs do not contain a PB1 domain at all, ARF3, ARF13, and ARF17, and several
17 more have lost the conserved acidic or basic residues in the PB1 domain, suggesting they
18 may be reduced to a single interaction domain. Several ARFs additionally have an expanded
19 conserved region within the DNA-binding domain, of unknown function. The majority of
20 domain variation among ARFs occurs in the large B-class subfamily. The liverwort
21 *Marchantia polymorpha* has a single representative ARF of each class (Flores-Sandoval,
22 Eklund, and Bowman 2015). The expansion of these classes in flowering plants is the result
23 of both whole genome and tandem duplication events (Remington et al. 2004). The growth
24 of the ARF family may have allowed for the expansion of the quantity and complexity of loci
25 regulated by the ARFs and subsequent expansion in their regulation of developmental
26 processes (Mutte et al. 2018).

27 Class A ARFs are the most well-studied ARF subfamily—the five family members all act as
28 transcriptional activators and have well-characterized, distinct developmental targets.
29 Overall the diversity of class A *ARF*s was generally low, especially compared to the class B
30 and C *ARF*s (Figure 11), suggesting that class A *ARF*s are central to auxin signal
31 transduction and plant development. Analysis of class A *ARF* nonsynonymous diversity
32 suggests that the majority of these *ARF*s are highly functionally conserved, with π_N/π_S
33 values much lower than 1 with the exception of *ARF19*, with π_N/π_S value of 1.8. Comparing
34 diversity within sister pairs, there is a similar trade-off as seen in most *IAA* sister pairs,
35 with one sister being highly conserved and the other more divergent. *ARF19* and *ARF8* are
36 the more divergent class A *ARF*s, with π_N/π_S values at least three time those of their sisters,
37 *ARF7* and *ARF6* respectively. This may suggest that ARF6 and ARF7 serve more essential
38 purposes in plant development.
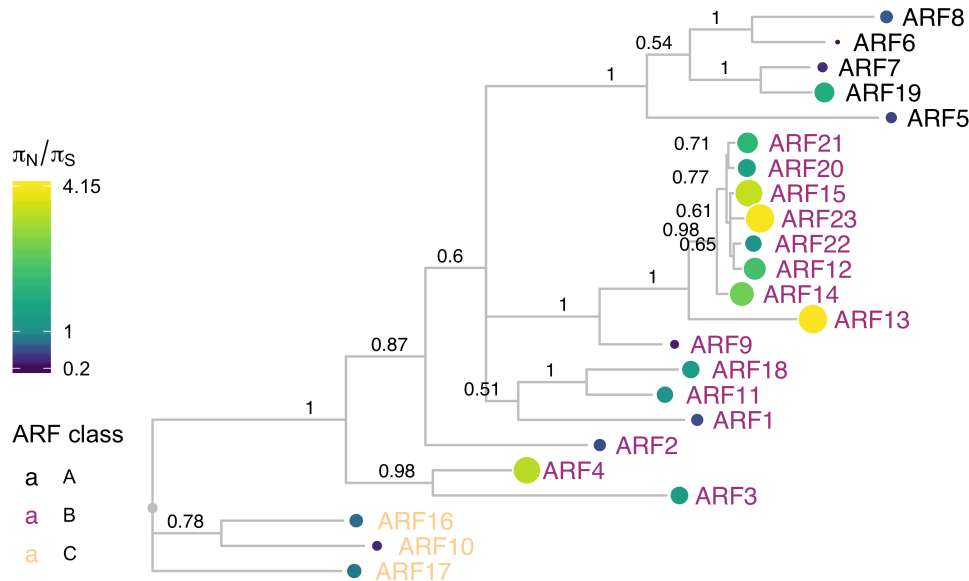
*Figure 11 **ARF protein sequence tree mapped with π_N/π_S.** Protein sequences were aligned with DECIPHER (Wright 2015) and low information content regions were masked with Aliscore (Kück et al. 2010) prior to inferring a phylogeny with MrBayes (Ronquist and Huelsenbeck 2003). Tips of the tree are mapped with circles of diameter proportional to π_N/π_S and also are colored according to π_N/π_S. Nodes are labeled with the poster probability of monophyly.*

For all class A *ARF*s, the middle region of the protein was the predominant high diversity region (Figure 12). In the analyzed natural variation, ARF7 had several expansions of polyglutamine sequences in the middle region. Polyglutamine regions are known to readily expand and contract throughout evolutionary time due to replication error, and variation in polyglutamine length can be acted on by natural selection and have phenotypic consequences (Press, Carlson, and Queitsch 2014). The ARF DNA-binding domain had very few, low-diversity missense mutations, as did the critical residues of the PB1 domain. Considering the necessity of their conserved functions, the low level of variation in these key DNA and protein-protein interaction domains is expected.

1
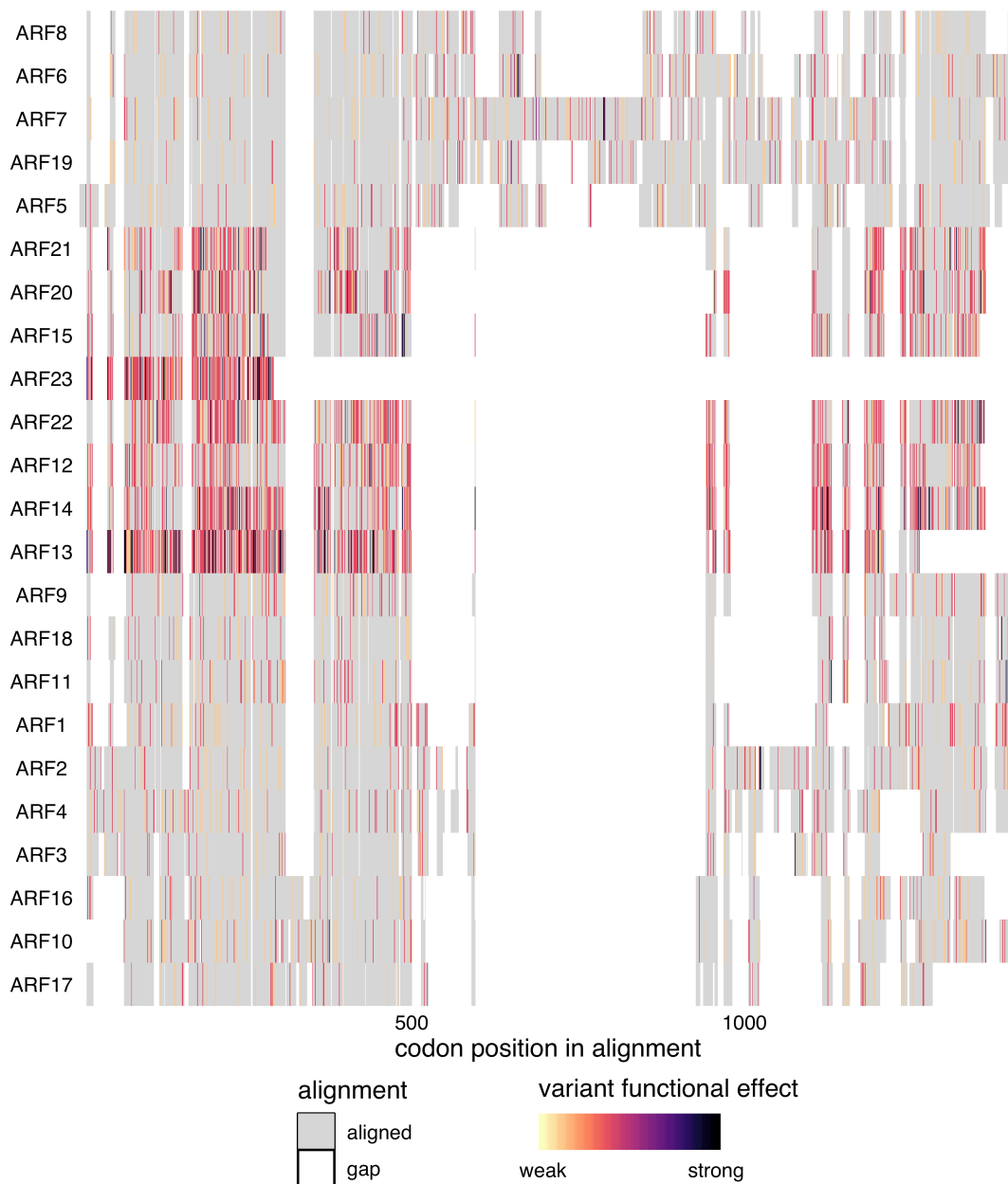
Figure 12 **Alignment of the full ARF family.** *Protein sequences were aligned with DECIPHER (Wright 2015) and variants were mapped to this alignment and colored according to the predicted functional effect of the allele of strongest effect at that position, with light colors having weaker effects on function and darker colors stronger effects. Red indicates missense variants. Color scale is explained in Methods.*

Many of the class B *ARF*s have very high π_N/π_S ratios relative to the other *ARF*s. ARF23 has a truncated DNA-binding domain and had a high π_N/π_S value of 4.1. ARF13 has many high-diversity nonsense variants and lacks a C-terminal PB1 domain. This high level of diversity, prevelance of high-frequency nonsense variants and frequent loss of critical domains, may suggest that several genes in this class are undergoing pseudogenization.

26

There are also a few highly conserved class B *ARF*s. The high conservation of *ARF1* and *ARF2* is expected as they play critical, redundant roles in senescence and abscission (Ellis et al. 2005). Little is known about *ARF9* however, and its low nonsynonymous diversity maybe worthy of investigation.

Class C ARFs show low nucleotide diversity scores, with all π_N/π_S values substantially lower than 1. *ARF16* was the most conserved, whereas its clade members (*ARF10*, *ARF17*) had scores at least four times higher. Structurally, all three members of Class C ARFs contain a canonical B3 DNA-binding domain, but only ARF10 and ARF16 contain a PB1 domain. The DNA binding domains exhibit overall low diversity. Of the PB1 domain containing class C ARFs, ARF16 exhibits several missense variants which are sporadically distributed, in contrast to the conserved PB1 domain of ARF10. This conservation in the PB1 domain of ARF10 and the DBD of ARF16 may suggest subfunctionalization in this family.

References

Alexandre, Cristina M., James R. Urton, Ken Jean-Baptiste, John Huddleston, Michael W. Dorrity, Josh T. Cuperus, Alessandra M. Sullivan, et al. 2018. "Complex Relationships Between Chromatin Accessibility, Sequence Divergence, and Gene Expression in Arabidopsis Thaliana." *Molecular Biology and Evolution* 35 (4): 837–54. doi:10.1093/molbev/msx326.

Allaire, JJ, Kevin Ushey, and Yuan Tang. 2018. *Reticulate: Interface to 'Python'*. https://CRAN.R-project.org/package=reticulate.

Allaire, JJ, Yihui Xie, Jonathan McPherson, Javier Luraschi, Kevin Ushey, Aron Atkins, Hadley Wickham, Joe Cheng, and Winston Chang. 2018. *Rmarkdown: Dynamic Documents for R*. https://CRAN.R-project.org/package=rmarkdown.

Aphalo, Pedro J. 2018a. *Gginnards: Explore the Innards of 'Ggplot2' Objects*. https://CRAN.R-project.org/package=gginnards.

———. 2018b. *Ggpmisc: Miscellaneous Extensions to 'Ggplot2'*. https://CRAN.R-project.org/package=ggpmisc.

Arnold, Jeffrey B. 2018. *Ggthemes: Extra Themes, Scales and Geoms for 'Ggplot2'*. https://CRAN.R-project.org/package=ggthemes.

Atwell, Susanna, Yu S. Huang, Bjarni J. Vilhjálmsson, Glenda Willems, Matthew Horton, Yan Li, Dazhe Meng, et al. 2010. "Genome-Wide Association Study of 107 Phenotypes in Arabidopsis Thaliana Inbred Lines." *Nature* 465 (7298): 627–31. doi:10.1038/nature08800.

Bache, Stefan Milton, and Hadley Wickham. 2014. *Magrittr: A Forward-Pipe Operator for R*. https://CRAN.R-project.org/package=magrittr.

Boer, D. Roeland, Alejandra Freire-Rios, Willy A. M. van den Berg, Terrens Saaki, Iain W. Manfield, Stefan Kepinski, Irene López-Vidrieo, et al. 2014. "Structural Basis for DNA Binding Specificity by the Auxin-Dependent ARF Transcription Factors." *Cell* 156 (3): 577–89. doi:10.1016/j.cell.2013.12.027.

Borevitz, Justin O., Samuel P. Hazen, Todd P. Michael, Geoffrey P. Morris, Ivan R. Baxter, Tina T. Hu, Huaming Chen, et al. 2007. "Genome-Wide Patterns of Single-Feature Polymorphism in Arabidopsis Thaliana." *Proceedings of the National Academy of Sciences of the United States of America* 104 (29): 12057–62. doi:10.1073/pnas.0705323104.

Calderón Villalobos, Luz Irina A., Sarah Lee, Cesar De Oliveira, Anthony Ivetac, Wolfgang Brandt, Lynne Armitage, Laura B. Sheard, et al. 2012. "A Combinatorial Tir1/AFB-Aux/IAA Co-Receptor System for Differential Sensing of Auxin." *Nat Chem Biol* 8 (5): 477–85. doi:10.1038/nchembio.926.

Cheng, Chia-Yi, Vivek Krishnakumar, Agnes P. Chan, Françoise Thibaud-Nissen, Seth Schobel, and Christopher D. Town. 2017. "Araport11: A Complete Reannotation of the Arabidopsis Thaliana Reference Genome." *The Plant Journal* 89 (4): 789–804. doi:10.1111/tpj.13415.

Clark, Richard M., Gabriele Schweikert, Christopher Toomajian, Stephan Ossowski, Georg Zeller, Paul Shinn, Norman Warthmann, et al. 2007. "Common Sequence Polymorphisms Shaping Genetic Diversity in Arabidopsis Thaliana." *Science* 317 (5836): 338–42. doi:10.1126/science.1138632.

Delker, Carolin, Yvonne Pöschl, Anja Raschke, Kristian Ullrich, Stefan Ettingshausen, Valeska Hauptmann, Ivo Grosse, and Marcel Quint. 2010. "Natural Variation of Transcriptional Auxin Response Networks in Arabidopsis Thaliana." *The Plant Cell* 22 (7): 2184–2200. doi:10.1105/tpc.110.073957.

Dezfulian, Mohammad H., Espanta Jalili, Don Karl A. Roberto, Britney L. Moss, Kerry Khoo, Jennifer L. Nemhauser, and William L. Crosby. 2016. "Oligomerization of SCF Tir1 Is Essential for Aux/IAA Degradation and Auxin Signaling in Arabidopsis." *PLOS Genet* 12 (9): e1006301. doi:10.1371/journal.pgen.1006301.

Dharmasiri, Nihal, Sunethra Dharmasiri, Dolf Weijers, Esther Lechner, Masashi Yamada, Lawrence Hobbie, Jasmin S. Ehrismann, Gerd Jürgens, and Mark Estelle. 2005. "Plant Development Is Regulated by a Family of Auxin Receptor F Box Proteins." *Developmental Cell* 9 (1): 109–19. doi:10.1016/j.devcel.2005.05.014.

Ellis, Christine M., Punita Nagpal, Jeffery C. Young, Gretchen Hagen, Thomas J. Guilfoyle, and Jason W. Reed. 2005. "AUXIN RESPONSE Factor1 and AUXIN RESPONSE Factor2 Regulate Senescence and Floral Organ Abscission in Arabidopsis Thaliana." *Development* 132 (20): 4563–74. doi:10.1242/dev.02012.

Firnberg, Elad, and Marc Ostermeier. 2013. "The Genetic Code Constrains yet Facilitates Darwinian Evolution." *Nucleic Acids Research* 41 (15): 7420–8. doi:10.1093/nar/gkt536.

Flores-Sandoval, Eduardo, D. Magnus Eklund, and John L. Bowman. 2015. "A Simple Auxin Transcriptional Response System Regulates Multiple Morphogenetic Processes in the Liverwort Marchantia Polymorpha." *PLOS Genetics* 11 (5): e1005207. doi:10.1371/journal.pgen.1005207.

Garnier, Simon. 2018a. *Viridis: Default Color Maps from 'Matplotlib'.* https://CRAN.R-project.org/package=viridis.

———. 2018b. *ViridisLite: Default Color Maps from 'Matplotlib' (Lite Version).* https://CRAN.R-project.org/package=viridisLite.

Gasperini, Molly, Lea Starita, and Jay Shendure. 2016. "The Power of Multiplexed Functional Analysis of Genetic Variants." *Nature Protocols* 11 (10): 1782–7. doi:10.1038/nprot.2016.135.

Guilfoyle, Tom J., and Gretchen Hagen. 2007. "Auxin Response Factors." *Current Opinion in Plant Biology*, Cell signalling and gene regulationedited by jian-kang zhu and ko shimamoto, 10 (5): 453–60. doi:10.1016/j.pbi.2007.08.014.

———. 2012. "Getting a Grasp on Domain III/IV Responsible for Auxin Response FactorIAA Protein Interactions." *Plant Science* 190 (July): 82–88. doi:10.1016/j.plantsci.2012.04.003.

Guseman, Jessica M., Antje Hellmuth, Amy Lanctot, Tamar P. Feldman, Britney L. Moss, Eric Klavins, Luz Irina A. Calderón Villalobos, and Jennifer L. Nemhauser. 2015. "Auxin-Induced Degradation Dynamics Set the Pace for Lateral Root Development." *Development* 142 (5): 905–9. doi:10.1242/dev.117234.

Hamm, Morgan O., and R. Clay Wright. 2018. *R1001genomes: Access and Analyze the 1001 Genomes Arabidopsis Resequencing Dataset.*

Havens, Kyle A., Jessica M. Guseman, Seunghee S. Jang, Edith Pierre-Jerome, Nick Bolten, Eric Klavins, and Jennifer L. Nemhauser. 2012. "A Synthetic Approach Reveals Extensive Tunability of Auxin Signaling." *Plant Physiology* 160 (1): 135–42. doi:10.1104/pp.112.202184.

Heibl, Christoph. 2014. *Ips: Interfaces to Phylogenetic Software in R.* https://CRAN.R-project.org/package=ips.

Henry, Lionel, and Hadley Wickham. 2018. *Purrr: Functional Programming Tools.* https://CRAN.R-project.org/package=purrr.

Hughes, Austin L. 1999. *Adaptive Evolution of Genes and Genomes.* Oxford University Press.

Hughes, Austin L., Jonathan A. Green, Juana M. Garbayo, and R. Michael Roberts. 2000. "Adaptive Diversification Within a Large Family of Recently Duplicated, Placentally Expressed Genes." *Proceedings of the National Academy of Sciences of the United States of America* 97 (7): 3319–23.

1 Ihaka, Ross, Paul Murrell, Kurt Hornik, Jason C. Fisher, Reto Stauffer, and Achim Zeileis.
2 2016. *Colorspace: Color Space Manipulation*. https://CRAN.R-
3 project.org/package=colorspace.

4 Ito, Jun, Hidehiro Fukaki, Makoto Onoda, Lin Li, Chuanyou Li, Masao Tasaka, and Masahiko
5 Furutani. 2016. "Auxin-Dependent Compositional Change in Mediator in Arf7- and Arf19-
6 Mediated Transcription." *Proceedings of the National Academy of Sciences*, May, 201600739.
7 doi:10.1073/pnas.1600739113.

8 Jacob, François. 1977. "Evolution and Tinkering." *Science* 196 (4295): 1161–6.

9 Joly-Lopez, Zoé, Jonathan M Flowers, and Michael D Purugganan. 2016. "Developing Maps
10 of Fitness Consequences for Plant Genomes." *Current Opinion in Plant Biology*, SI: 30:
11 Genome studies and molecular genetics, 30 (April): 101–7. doi:10.1016/j.pbi.2016.02.008.

12 Joshi, Hiren J., Katy M. Christiansen, Joffrey Fitz, Jun Cao, Anna Lipzen, Joel Martin, A.
13 Michelle Smith-Moritz, et al. 2012. "1001 Proteomes: A Functional Proteomics Portal for
14 the Analysis of Arabidopsis Thaliana Accessions." *Bioinformatics* 28 (10): 1303–6.
15 doi:10.1093/bioinformatics/bts133.

16 Ke, Jiyuan, Honglei Ma, Xin Gu, Adam Thelen, Joseph S. Brunzelle, Jiayang Li, H. Eric Xu, and
17 Karsten Melcher. 2015. "Structural Basis for Recognition of Diverse Transcriptional
18 Repressors by the TOPLESS Family of Corepressors." *Science Advances* 1 (6): e1500107.
19 doi:10.1126/sciadv.1500107.

20 Kliebenstein, Daniel J. 2008. "A Role for Gene Duplication and Natural Variation of Gene
21 Expression in the Evolution of Metabolism." *PLOS ONE* 3 (3): e1838.
22 doi:10.1371/journal.pone.0001838.

23 Korasick, David A., Corey S. Westfall, Soon Goo Lee, Max H. Nanao, Renaud Dumas, Gretchen
24 Hagen, Thomas J. Guilfoyle, Joseph M. Jez, and Lucia C. Strader. 2014. "Molecular Basis for
25 AUXIN RESPONSE FACTOR Protein Interaction and the Control of Auxin Response
26 Repression." *Proceedings of the National Academy of Sciences* 111 (14): 5427–32.
27 doi:10.1073/pnas.1400074111.

28 Kück, Patrick, Karen Meusemann, Johannes Dambach, Birthe Thormann, Björn M. von
29 Reumont, Johann W. Wägele, and Bernhard Misof. 2010. "Parametric and Non-Parametric
30 Masking of Randomness in Sequence Alignments Can Be Improved and Leads to Better
31 Resolved Trees." *Frontiers in Zoology* 7 (March): 10. doi:10.1186/1742-9994-7-10.

32 Long, Jeff A., Carolyn Ohno, Zachery R. Smith, and Elliot M. Meyerowitz. 2006. "TOPLESS
33 Regulates Apical Embryonic Fate in Arabidopsis." *Science* 312 (5779): 1520–3.
34 doi:10.1126/science.1123841.

35 Long, Quan, Fernando A Rabanal, Dazhe Meng, Christian D Huber, Ashley Farlow, Alexander
36 Platzer, Qingrun Zhang, et al. 2013. "Massive Genomic Variation and Strong Selection in
37 Arabidopsis Thaliana Lines from Sweden." *Nature Genetics* 45 (8): 884–90.
38 doi:10.1038/ng.2678.

1   Ma, Honglei, Jingbo Duan, Jiyuan Ke, Yuanzheng He, Xin Gu, Ting-Hai Xu, Hong Yu, et al.
2   2017. "A D53 Repression Motif Induces Oligomerization of TOPLESS Corepressors and
3   Promotes Assembly of a Corepressor-Nucleosome Complex." *Science Advances* 3 (6).
4   doi:10.1126/sciadv.1601217.

5   Martin-Arevalillo, Raquel, Max H. Nanao, Antoine Larrieu, Thomas Vinos-Poyo, David Mast,
6   Carlos Galvan-Ampudia, Géraldine Brunoud, Teva Vernoux, Renaud Dumas, and François
7   Parcy. 2017. "Structure of the Arabidopsis TOPLESS Corepressor Provides Insight into the
8   Evolution of Transcriptional Repression." *Proceedings of the National Academy of Sciences*,
9   July, 201703054. doi:10.1073/pnas.1703054114.

10   Matreyek, Kenneth A., Jason J. Stephany, and Douglas M. Fowler. 2017. "A Platform for
11   Functional Assessment of Large Variant Libraries in Mammalian Cells." *Nucleic Acids
12   Research* 45 (11): e102. doi:10.1093/nar/gkx183.

13   Melamed, Daniel, David L. Young, Christina R. Miller, and Stanley Fields. 2015. "Combining
14   Natural Sequence Variation with High Throughput Mutational Data to Reveal Protein
15   Interaction Sites." *PLoS Genet* 11 (2): e1004918. doi:10.1371/journal.pgen.1004918.

16   Michael, Todd P., Florian Jupe, Felix Bemm, S. Timothy Motley, Justin P. Sandoval, Christa
17   Lanz, Olivier Loudet, Detlef Weigel, and Joseph R. Ecker. 2018. "High Contiguity Arabidopsis
18   Thaliana Genome Assembly with a Single Nanopore Flow Cell." *Nature Communications* 9
19   (1): 541. doi:10.1038/s41467-018-03016-2.

20   Mutte, Sumanth K., Hirotaka Kato, Carl Rothfels, Michael Melkonian, Gane Ka-Shu Wong,
21   and Dolf Weijers. 2018. "Origin and Evolution of the Nuclear Auxin Response System." *eLife*
22   7 (March): e33399. doi:10.7554/eLife.33399.

23   Müller, Kirill. 2018. *Bindrcpp: An 'Rcpp' Interface to Active Bindings*. https://CRAN.R-
24   project.org/package=bindrcpp.

25   Müller, Kirill, and Hadley Wickham. 2018. *Tibble: Simple Data Frames*. https://CRAN.R-
26   project.org/package=tibble.

27   Müller, Kirill, Hadley Wickham, David A. James, and Seth Falcon. 2018. *RSQLite: 'SQLite'
28   Interface for R*. https://CRAN.R-project.org/package=RSQLite.

29   Nanao, Max H., Thomas Vinos-Poyo, Géraldine Brunoud, Emmanuel Thévenon, Meryl
30   Mazzoleni, David Mast, Stéphanie Lainé, et al. 2014. "Structural Basis for Oligomerization of
31   Auxin Transcriptional Regulators." *Nature Communications* 5: 3617.
32   doi:10.1038/ncomms4617.

33   Nei, M, and W H Li. 1979. "Mathematical Model for Studying Genetic Variation in Terms of
34   Restriction Endonucleases." *Proceedings of the National Academy of Sciences of the United
35   States of America* 76 (10): 5269–73.

36   Nelson, Chase W., Louise H. Moncla, and Austin L. Hughes. 2015. "SNPGenie: Estimating
37   Evolutionary Parameters to Detect Natural Selection Using Pooled Next-Generation
38   Sequencing Data." *Bioinformatics* 31 (22): 3709–11. doi:10.1093/bioinformatics/btv449.

Neuwirth, Erich. 2014. *RColorBrewer: ColorBrewer Palettes*. https://CRAN.R-project.org/package=RColorBrewer.

Nordborg, Magnus, Tina T Hu, Yoko Ishino, Jinal Jhaveri, Christopher Toomajian, Honggang Zheng, Erica Bakker, et al. 2005. "The Pattern of Polymorphism in Arabidopsis Thaliana." *PLoS Biol* 3 (7): e196. doi:10.1371/journal.pbio.0030196.

Overvoorde, Paul J., Yoko Okushima, José M. Alonso, April Chan, Charlie Chang, Joseph R. Ecker, Beth Hughes, et al. 2005. "Functional Genomic Analysis of the AUXIN/INDOLE-3-ACETIC ACID Gene Family Members in Arabidopsis Thaliana." *The Plant Cell* 17 (12): 3282–3300. doi:10.1105/tpc.105.036723.

Pagès, H., P. Aboyoun, and M. Lawrence. 2018. *IRanges: Infrastructure for Manipulating Intervals on Sequences*.

Pagès, H., P. Aboyoun, R. Gentleman, and S. DebRoy. 2018. *Biostrings: Efficient Manipulation of Biological Strings*.

Pagès, H., M. Lawrence, and P. Aboyoun. 2018. *S4Vectors: S4 Implementation of Vector-Like and List-Like Objects*.

Pagès, Hervé, and Patrick Aboyoun. 2018. *XVector: Representation and Manipulation of External Sequences*.

Paradis, Emmanuel, Simon Blomberg, Ben Bolker, Joseph Brown, Julien Claude, Hoa Sien Cuong, Richard Desper, et al. 2018. *Ape: Analyses of Phylogenetics and Evolution*. https://CRAN.R-project.org/package=ape.

Park, Briton, Matthew T. Rutter, Charles B. Fenster, V. Vaughan Symonds, Mark C. Ungerer, and Jeffrey P. Townsend. 2017. "Distributions of Mutational Effects and the Estimation of Directional Selection in Divergent Lineages of Arabidopsis Thaliana." *Genetics* 206 (4): 2105–17. doi:10.1534/genetics.116.199190.

Parry, G., L. I. Calderon-Villalobos, M. Prigge, B. Peret, S. Dharmasiri, H. Itoh, E. Lechner, W. M. Gray, M. Bennett, and M. Estelle. 2009. "Complex Regulation of the Tir1/AFB Family of Auxin Receptors." *Proceedings of the National Academy of Sciences* 106 (52): 22540–5. doi:10.1073/pnas.0911967106.

Pierre-Jerome, Edith, Britney L. Moss, Amy Lanctot, Amber Hageman, and Jennifer L. Nemhauser. 2016. "Functional Analysis of Molecular Interactions in Synthetic Auxin Response Circuits." *Proceedings of the National Academy of Sciences of the United States of America* 113 (40): 11354–9. doi:10.1073/pnas.1604379113.

Press, Maximilian O., Keisha D. Carlson, and Christine Queitsch. 2014. "The Overdue Promise of Short Tandem Repeat Variation for Heritability." *Trends in Genetics: TIG* 30 (11): 504–12. doi:10.1016/j.tig.2014.07.008.

Prigge, Michael J., Kathleen Greenham, Yi Zhang, Aaron Santner, Cristina Castillejo, Andrew M. Mutka, Ronan C. O'Malley, Joseph R. Ecker, Barbara N. Kunkel, and Mark Estelle. 2016.

"The Arabidopsis Auxin Receptor F-Box Proteins Afb4 and Afb5 Are Required for Response to the Synthetic Auxin Picloram." *G3: Genes|Genomes|Genetics* 6 (5): 1383–90. doi:10.1534/g3.115.025585.

R Core Team. 2018. *R: A Language and Environment for Statistical Computing*. Vienna, Austria: R Foundation for Statistical Computing. https://www.R-project.org/.

Remington, David L., Todd J. Vision, Thomas J. Guilfoyle, and Jason W. Reed. 2004. "Contrasting Modes of Diversification in the Aux/IAA and ARF Gene Families." *Plant Physiology* 135 (3): 1738–52. doi:10.1104/pp.104.039669.

Ronquist, F., and J. P. Huelsenbeck. 2003. "MrBayes 3: Bayesian Phylogenetic Inference Under Mixed Models." *Bioinformatics* 19 (12): 1572–4. doi:10.1093/bioinformatics/btg180.

Starita, Lea M., Nadav Ahituv, Maitreya J. Dunham, Jacob O. Kitzman, Frederick P. Roth, Georg Seelig, Jay Shendure, and Douglas M. Fowler. 2017. "Variant Interpretation: Functional Assays to the Rescue." *The American Journal of Human Genetics* 101 (3): 315–25. doi:10.1016/j.ajhg.2017.07.014.

Szemenyei, Heidi, Mike Hannon, and Jeff A. Long. 2008. "TOPLESS Mediates Auxin-Dependent Transcriptional Repression During Arabidopsis Embryogenesis." *Science* 319 (5868): 1384–6. doi:10.1126/science.1151461.

Tan, Xu, Luz Irina A. Calderon-Villalobos, Michal Sharon, Changxue Zheng, Carol V. Robinson, Mark Estelle, and Ning Zheng. 2007. "Mechanism of Auxin Perception by the Tir1 Ubiquitin Ligase." *Nature* 446 (7136): 640–5. doi:10.1038/nature05731.

Team, The Bioconductor Dev. 2018. *BiocGenerics: S4 Generic Functions for Bioconductor*.

Temple Lang, Duncan, and the CRAN Team. 2018. *XML: Tools for Parsing and Generating Xml Within R and S-Plus*. https://CRAN.R-project.org/package=XML.

The Arabidopsis Genome Initiative. 2000. "Analysis of the Genome Sequence of the Flowering Plant *Arabidopsis Thaliana*." *Nature* 408 (6814): 796–815. doi:10.1038/35048692.

Tiwari, Shiv B., Gretchen Hagen, and Tom J. Guilfoyle. 2004. "Aux/IAA Proteins Contain a Potent Transcriptional Repression Domain." *The Plant Cell* 16 (2): 533–43. doi:10.1105/tpc.017384.

Ulmasov, T., J. Murfett, G. Hagen, and T. J. Guilfoyle. 1997. "Aux/IAA Proteins Repress Expression of Reporter Genes Containing Natural and Highly Active Synthetic Auxin Response Elements." *The Plant Cell Online* 9 (11): 1963–71. doi:10.1105/tpc.9.11.1963.

Waese, Jamie, Jim Fan, Asher Pasha, Hans Yu, Geoffrey Fucile, Ruian Shi, Matthew Cumming, et al. 2017. "ePlant: Visualizing and Exploring Multiple Levels of Data for Hypothesis Generation in Plant Biology." *The Plant Cell* 29 (8): 1806–21. doi:10.1105/tpc.17.00073.

Wagih, Omar. 2017. *Ggseqlogo: A 'Ggplot2' Extension for Drawing Publication-Ready Sequence Logos.* https://CRAN.R-project.org/package=ggseqlogo.

Wang, Wensheng, Ramil Mauleon, Zhiqiang Hu, Dmytro Chebotarov, Shuaishuai Tai, Zhichao Wu, Min Li, et al. 2018. "Genomic Variation in 3,010 Diverse Accessions of Asian Cultivated Rice." *Nature* 557 (7703): 43. doi:10.1038/s41586-018-0063-9.

Weigel, Detlef, and Richard Mott. 2009. "The 1001 Genomes Project for Arabidopsis Thaliana." *Genome Biology* 10 (5): 107. doi:10.1186/gb-2009-10-5-107.

Whitehead, Timothy A, Aaron Chevalier, Yifan Song, Cyrille Dreyfus, Sarel J Fleishman, Cecilia De Mattos, Chris A Myers, et al. 2012. "Optimization of Affinity, Specificity and Function of Designed Influenza Inhibitors Using Deep Sequencing." *Nature Biotechnology* 30 (6): 543–48. doi:10.1038/nbt.2214.

Wickham, Hadley. 2016. *Plyr: Tools for Splitting, Applying and Combining Data.* https://CRAN.R-project.org/package=plyr.

———. 2017a. *Reshape2: Flexibly Reshape Data: A Reboot of the Reshape Package.* https://CRAN.R-project.org/package=reshape2.

———. 2017b. *Tidyverse: Easily Install and Load the 'Tidyverse'.* https://CRAN.R-project.org/package=tidyverse.

———. 2018a. *Forcats: Tools for Working with Categorical Variables (Factors).* https://CRAN.R-project.org/package=forcats.

———. 2018b. *Scales: Scale Functions for Visualization.* https://CRAN.R-project.org/package=scales.

———. 2018c. *Stringr: Simple, Consistent Wrappers for Common String Operations.* https://CRAN.R-project.org/package=stringr.

Wickham, Hadley, and Lionel Henry. 2018. *Tidyr: Easily Tidy Data with 'Spread()' and 'Gather()' Functions.* https://CRAN.R-project.org/package=tidyr.

Wickham, Hadley, Winston Chang, Lionel Henry, Thomas Lin Pedersen, Kohske Takahashi, Claus Wilke, and Kara Woo. 2018. *Ggplot2: Create Elegant Data Visualisations Using the Grammar of Graphics.* https://CRAN.R-project.org/package=ggplot2.

Wickham, Hadley, Romain François, Lionel Henry, and Kirill Müller. 2018. *Dplyr: A Grammar of Data Manipulation.* https://CRAN.R-project.org/package=dplyr.

Wickham, Hadley, Jim Hester, and Romain Francois. 2017. *Readr: Read Rectangular Text Data.* https://CRAN.R-project.org/package=readr.

Winkler, Martin, Michael Niemeyer, Antje Hellmuth, Philipp Janitza, Gideon Christ, Sophia L. Samodelov, Verona Wilde, et al. 2017. "Variation in Auxin Sensing Guides AUX/IAA Transcriptional Repressor Ubiquitylation and Destruction." *Nature Communications* 8 (June): 15706. doi:10.1038/ncomms15706.

Wright, Erik. 2018. *DECIPHER: Tools for Curating, Analyzing, and Manipulating Biological Sequences.*

Wright, Erik S. 2015. "DECIPHER: Harnessing Local Sequence Context to Improve Protein Multiple Sequence Alignment." *BMC Bioinformatics* 16 (October): 322. doi:10.1186/s12859-015-0749-z.

Wright, R. Clay, Mollye L. Zahler, Stacey R. Gerben, and Jennifer L. Nemhauser. 2017. "Insights into the Evolution and Function of Auxin Signaling F-Box Proteins in Arabidopsis Thaliana Through Synthetic Analysis of Natural Variants." *Genetics* 207 (2): 583–91. doi:10.1534/genetics.117.300092.

Wu, Miin-Feng, Nobutoshi Yamaguchi, Jun Xiao, Bastiaan Bargmann, Mark Estelle, Yi Sang, and Doris Wagner. 2015. "Auxin-Regulated Chromatin Switch Directs Acquisition of Flower Primordium Founder Fate." *eLife* 4 (October): e09269. doi:10.7554/eLife.09269.

Xie, Yihui. 2018a. *Bookdown: Authoring Books and Technical Documents with R Markdown.* https://CRAN.R-project.org/package=bookdown.

———. 2018b. *DT: A Wrapper of the Javascript Library 'Datatables'.* https://CRAN.R-project.org/package=DT.

———. 2018c. *Knitr: A General-Purpose Package for Dynamic Report Generation in R.* https://CRAN.R-project.org/package=knitr.

Yu, Guangchuang. 2018. *Treeio: Base Classes and Functions for Phylogenetic Tree Input and Output.* https://guangchuangyu.github.io/software/treeio.

Yu, Guangchuang, and Tommy Tsan-Yuk Lam. 2018. *Ggtree: An R Package for Visualization and Annotation of Phylogenetic Trees with Their Covariates and Other Associated Data.* https://guangchuangyu.github.io/software/ggtree.

Yu, Hong, Yi Zhang, Britney L. Moss, Bastiaan O. R. Bargmann, Renhou Wang, Michael Prigge, Jennifer L. Nemhauser, and Mark Estelle. 2015. "Untethering the Tir1 Auxin Receptor from the SCF Complex Increases Its Stability and Inhibits Auxin Response." *Nature Plants* 1 (3): 14030. doi:10.1038/nplants.2014.30.

Zhou, Zhengkui, Yu Jiang, Zheng Wang, Zhiheng Gou, Jun Lyu, Weiyu Li, Yanjun Yu, et al. 2015. "Resequencing 302 Wild and Cultivated Accessions Identifies Genes Related to Domestication and Improvement in Soybean." *Nature Biotechnology* 33 (4): 408–14. doi:10.1038/nbt.3096.